Chapter 4
Light-Dressed Spectroscopy of Molecules

Tamás Szidarovszky, Gábor J. Halász, Attila G. Császár, and Ágnes Vibók

Abstract We present a theoretical approach for simulating rovibronic spectra of molecules dressed by medium-intensity laser fields. Numerical results, obtained through the formalism described, are presented for the homonuclear diatomic molecule Na_2, a system suitable for demonstrating and understanding various aspects of light-dressed spectroscopy. We discuss the physical origin of the peaks in the light-dressed spectrum of Na_2 and investigate the light-dressed spectrum in terms of its dependence on the dressing field's intensity and wavelength, temperature, and the turn-on time of the dressing field. The possibility of using light-dressed spectroscopy to derive field-free spectroscopic quantities is also addressed.

4.1 Introduction

Despite the long history of spectroscopy, spanning two centuries, new approaches and methods are being developed in it to this day [1]. This is principally due to the great success of atomic and molecular spectroscopy, both in fundamental research

T. Szidarovszky (✉) · A. G. Császár
Institute of Chemistry, Eötvös Loránd University and MTA-ELTE Complex Chemical Systems Research Group, Pázmány Péter sétány 1/A, Budapest 1117, Hungary
e-mail: tamas821@caesar.elte.hu

A. G. Császár
e-mail: csaszarag@caesar.elte.hu

G. J. Halász
Department of Information Technology, University of Debrecen, PO Box 400, Debrecen 4002, Hungary
e-mail: halasz.gabor@inf.unideb.hu

Á. Vibók
Department of Theoretical Physics, University of Debrecen, PO Box 400, Debrecen 4002, Hungary
e-mail: vibok@phys.unideb.hu

ELI-ALPS, ELI-HU Non-Profit Ltd., Wolfgang Sandner utca 3, Szeged H-6728, Hungary

K. Yamanouchi and D. Charalambidis (eds.), *Progress in Ultrafast Intense Laser Science XV*, Topics in Applied Physics 136,
https://doi.org/10.1007/978-3-030-47098-2_4

and in practical applications, as well as to the remarkable advances in the available experimental techniques and light sources. For example, the development of frequency-comb techniques [2–5] facilitates extremely precise and accurate measurements in the frequency domain, while the development of ultrashort and intense pulsed laser technologies [6, 7] allows for time-resolved spectroscopy on femtosecond or even attosecond [7, 8] timescales.

An often utilized technique of modern spectroscopic methods is the use of two (or more) light pulses. Some of these pulses act as so-called pump pulses, which induce specific changes in the system. Subsequent, so-called probe pulses are used then to measure, directly or indirectly, the changes induced by the pump pulse(s). If the duration of both the pump and the probe pulses is short with respect to the processes investigated, repeating the experiment with varying time delays between the pulses can lead to time-resolved dynamical information [9, 10] or to multidimensional and/or high-resolution spectra [11, 12]. If the pump and probe pulses overlap in time, the signal recorded by the probe pulse does not represent the field-free system, but rather the so-called field-dressed or light-dressed system [13, 14], where the pump pulse acts as the dressing field. If both the pump and the probe pulses are long with respect to the timescales of the processes investigated, one obtains static spectral properties of the light-dressed system. In this chapter we investigate such static spectra of light-dressed systems and henceforth call it *light-dressed spectroscopy*.

For atomic systems the theoretical and experimental methods for investigating optical transitions between light-dressed states is well developed [13]. As to molecules, the concept of light-dressed electronic states, also called light-dressed potentials, has been utilized with considerable success to understand nuclear dynamics both in experimental and theoretical studies [15–23]. To some extent light-dressed rovibrational spectroscopy has been adopted for molecular systems. For example, inducing Autler–Townes-type splittings [24] of rotational transitions with microwave radiation has been used to deduce molecular parameters [25, 26] as well as to promote the spectral assignments of rovibronic levels [27].

In previous theoretical studies the rovibronic spectrum of light-dressed Na_2 was investigated in the context of how the presence of a light-induced conical intersection (LICI) [28, 29], generated by the dressing field, can be identified in the spectrum [30, 31]. In these works all rovibronic degrees of freedom are incorporated into the concept of light-dressed states and the modeling work is carried out for both the dressing field of laser radiation [30] and the quantized dressing field of a microscopic cavity mode [31]. In a separate paper, we provided a more general and detailed discussion on the computation and the properties of light-dressed spectra [32].

In this chapter we review in detail the theory of computing light-dressed spectra induced by laser fields and investigate certain aspects of light-dressed spectroscopy, including its unique properties on deriving spectroscopic information. Our discussion closely follows the one presented in [32].

4.2 Theoretical Approach

Our approach to compute light-dressed spectra of molecules is based on three well-defined steps. First, we compute all field-free molecular rovibronic states relevant to the light-induced processes. Second, using the field-free eigenstates as molecular basis functions, we determine the light-dressed states induced by a medium-intensity light field within the framework of Floquet theory [14, 33, 34]. Third, we compute the transitions between the light-dressed states, induced by a weak probe pulse.

In order to facilitate the required computations, we make the following assumptions: (1) Initially the molecule is in a field-free eigenstate in the gas phase. (2) The molecule is exposed to a medium-intensity dressing light, which is turned on adiabatically, i.e., its envelope varies much slower than the rovibronic timescales characterizing the molecule. (3) The probe pulse, introduced to record the static rovibronic spectrum of the light-dressed molecule, is weak and can be treated in a perturbative manner.

4.2.1 Determination of Light-Dressed States

4.2.1.1 General Considerations

In this section we review some aspects of the Floquet approach [14, 33, 34] which we use to compute the light-dressed states generated by a medium-intensity pump pulse. For a dressed Hamiltonian periodic in time t, such as

$$\hat{H}_{\mathrm{d}}(t) = \hat{H}_{\mathrm{mol}} + \hat{W}_1(t), \tag{4.1}$$

$$\hat{H}_{\mathrm{d}}(t+T) = \hat{H}_{\mathrm{d}}(t), \tag{4.2}$$

where $\hat{H}_{\mathrm{mol}}$ is the field-free molecular Hamiltonian, $T = 2\pi/\omega_1$ is the time period of the periodicity, and $\hat{W}_1(t)$ is the interaction between the molecule and the dressing field, the time-dependent Schrödinger equation (TDSE)

$$i\hbar\partial_t|\psi(t)\rangle = \hat{H}_{\mathrm{d}}(t)|\psi(t)\rangle \tag{4.3}$$

has the general solution

$$|\psi(t)\rangle = \sum_k c_k e^{-\frac{i}{\hbar}\varepsilon_k t}|\Phi_k(t)\rangle, \tag{4.4}$$

where ε_k are the so-called quasienergies, and $|\Phi_k(t)\rangle$ are the Floquet states (also called light-dressed states in our work). The Floquet states satisfy

$$|\Phi_k(t+T)\rangle = |\Phi_k(t)\rangle, \tag{4.5}$$

and

$$(\hat{H}_\mathrm{d}(t) - i\hbar\partial_t)|\Phi_k(t)\rangle = \hat{H}_\mathrm{F}(t)|\Phi_k(t)\rangle = \varepsilon_k|\Phi_k(t)\rangle. \tag{4.6}$$

As can be verified using (4.6), if ε_k is a quasienergy, then $\varepsilon_k + \hbar m\omega_1$ is also a quasienergy with a corresponding Floquet state $e^{im\omega_1 t}|\Phi_k(t)\rangle$, where m is an integer. As (4.4) demonstrates, such a shifted quasienergy does not represent a new physical state, because $\varepsilon_k + \hbar m\omega_1$ with $e^{im\omega_1 t}|\Phi_k(t)\rangle$ gives the same contribution to the wave function as ε_k with $|\Phi_k(t)\rangle$.

Because $|\Phi_k(t)\rangle$ are periodic in time, they can be expanded as a Fourier series,

$$|\Phi_k(t)\rangle = \sum_n |\varphi_{kn}\rangle e^{in\omega_1 t}. \tag{4.7}$$

Substituting (4.7) into (4.6) and assuming $\hat{W}_1(t) = -\mathbf{E}_1\hat{\boldsymbol{\mu}}\cos(\omega_1 t) = -\frac{1}{2}\mathbf{E}_1\hat{\boldsymbol{\mu}}(e^{i\omega_1 t} + e^{-i\omega_1 t})$, (4.6) becomes

$$\begin{aligned}(\hat{H}_\mathrm{mol} + \hbar n\omega_1)\sum_n |\varphi_{kn}\rangle e^{in\omega_1 t} - \frac{1}{2}\mathbf{E}_1\hat{\boldsymbol{\mu}}\sum_n |\varphi_{kn}\rangle(e^{i(n+1)\omega_1 t} + e^{i(n-1)\omega_1 t}) \\ = \varepsilon_k \sum_n |\varphi_{kn}\rangle e^{in\omega_1 t}.\end{aligned} \tag{4.8}$$

Multiplying (4.8) with $\frac{1}{T}e^{-im\omega_1 t}$ and integrating over the time period T leads to

$$(\hat{H}_\mathrm{mol} + \hbar m\omega_1)|\varphi_{km}\rangle - \frac{1}{2}\mathbf{E}_1\hat{\boldsymbol{\mu}}\big(|\varphi_{k,m-1}\rangle + |\varphi_{k,m+1}\rangle\big) = \varepsilon_k|\varphi_{km}\rangle. \tag{4.9}$$

The Fourier components $|\varphi_{km}\rangle$ can be further expressed as a linear combination of field-free rovibronic molecular eigenstates

$$|\varphi_{km}\rangle = \sum_{\alpha,v,J} C^{(k)}_{m,\alpha vJ}|\alpha vJ\rangle, \tag{4.10}$$

where α, v, and J represent electronic, vibrational, and rotational quantum numbers, respectively. Using the expansion of (4.10), (4.9) can be turned into the matrix eigenvalue problem

$$\sum_{n,\alpha,v,J} (\mathbf{H}_\mathrm{F})_{m\alpha' v' J', n\alpha vJ} C^{(k)}_{n,\alpha vJ} = \varepsilon_k C^{(k)}_{m,\alpha' v' J'}, \tag{4.11}$$

where

$$
\begin{aligned}
&(\mathbf{H}_{\mathrm{F}})_{m\alpha' v' J', n\alpha v J} \\
&\quad = \big(\langle \alpha' v' J' | \hat{H}_{\mathrm{mol}} | \alpha v J \rangle + \hbar m \omega_1 \delta_{\alpha\alpha'} \delta_{vv'} \delta_{JJ'}\big)\delta_{nm} \\
&\qquad -\frac{1}{2}\langle \alpha' v' J' | \mathbf{E}_1 \hat{\boldsymbol{\mu}} | \alpha v J \rangle \big(\delta_{n,m-1} + \delta_{n,m+1}\big).
\end{aligned} \tag{4.12}
$$

The pictorial representation of $\mathbf{H}_{\mathrm{F}}$ reads as

$$
\mathbf{H}_{\mathrm{F}} = \begin{bmatrix}
\ddots & \vdots & \vdots & \vdots & \vdots & \vdots & \vdots & \iddots \\
\cdots & \mathbf{H}_{\mathrm{A}} + \hbar\omega_1 \mathbf{I} & \boldsymbol{\lambda} & \mathbf{g}_{\mathrm{AA}} & \mathbf{g}_{\mathrm{AX}} & 0 & 0 & \cdots \\
\cdots & \boldsymbol{\lambda}^{\dagger} & \mathbf{H}_{\mathrm{X}} + \hbar\omega_1 \mathbf{I} & \mathbf{g}_{\mathrm{XA}} & \mathbf{g}_{\mathrm{XX}} & 0 & 0 & \cdots \\
\cdots & \mathbf{g}_{\mathrm{AA}}^{\dagger} & \mathbf{g}_{\mathrm{XA}}^{\dagger} & \mathbf{H}_{\mathrm{A}} & \boldsymbol{\lambda} & \mathbf{g}_{\mathrm{AA}} & \mathbf{g}_{\mathrm{AX}} & \cdots \\
\cdots & \mathbf{g}_{\mathrm{AX}}^{\dagger} & \mathbf{g}_{\mathrm{XX}}^{\dagger} & \boldsymbol{\lambda}^{\dagger} & \mathbf{H}_{\mathrm{X}} & \mathbf{g}_{\mathrm{XA}} & \mathbf{g}_{\mathrm{XX}} & \cdots \\
\cdots & 0 & 0 & \mathbf{g}_{\mathrm{AA}}^{\dagger} & \mathbf{g}_{\mathrm{XA}}^{\dagger} & \mathbf{H}_{\mathrm{A}} - \hbar\omega_1 \mathbf{I} & \boldsymbol{\lambda} & \cdots \\
\cdots & 0 & 0 & \mathbf{g}_{\mathrm{AX}}^{\dagger} & \mathbf{g}_{\mathrm{XX}}^{\dagger} & \boldsymbol{\lambda}^{\dagger} & \mathbf{H}_{\mathrm{X}} - \hbar\omega_1 \mathbf{I} & \cdots \\
\iddots & \vdots & \vdots & \vdots & \vdots & \vdots & \vdots & \ddots
\end{bmatrix}, \tag{4.13}
$$

where each row/column represents a different combination of the values for the α electronic and n Fourier indices of (4.12) (for the sake of simplicity, we assumed only two electronic states, labeled X and A, where X denotes the ground electronic state), and each matrix element in (4.13) is itself a matrix representation of different operators in the space of rovibrational states, i.e.,

$$
(\mathbf{H}_{\mathrm{A}})_{v'J',vJ} = \langle \mathrm{A} v' J' | \hat{H}_{\mathrm{mol}} | \mathrm{A} v J \rangle, \tag{4.14}
$$

$$
(\mathbf{H}_{\mathrm{X}})_{v'J',vJ} = \langle \mathrm{X} v' J' | \hat{H}_{\mathrm{mol}} | \mathrm{X} v J \rangle, \tag{4.15}
$$

$$
(\boldsymbol{\lambda})_{v'J',vJ} = \langle \mathrm{A} v' J' | \hat{H}_{\mathrm{mol}} | \mathrm{X} v J \rangle, \tag{4.16}
$$

and

$$
(\mathbf{g}_{\alpha\beta})_{v'J',vJ} = -\frac{1}{2}\langle \alpha v' J' | \mathbf{E}_1 \hat{\boldsymbol{\mu}} | \beta v J \rangle, \tag{4.17}
$$

and $\mathbf{I}$ is the identity matrix. $\mathbf{H}_{\mathrm{A}}$ and $\mathbf{H}_{\mathrm{X}}$ can be thought of as the rovibrational Hamiltonians in the adiabatic electronic states A and X, respectively, while $\boldsymbol{\lambda}$ accounts for intrinsic nonadiabatic couplings between the X and A electronic states. The coupling induced by the dressing field is represented by $\mathbf{g}_{\alpha\beta}$.

After solving (4.11), by diagonalizing the matrix of (4.13), the light-dressed states can be written with the help of (4.7) and (4.10) as

$$
|\Phi_k\rangle = \sum_{n,\alpha,v,J} C^{(k)}_{n,\alpha v J} |\alpha v J\rangle |n\rangle, \tag{4.18}
$$

where we adopt the notation called "*Floquet-state nomenclature*" [33], in which $\langle t|n\rangle = e^{in\omega_1 t}$ and $\omega_1 = 2\pi/T$ with $|\Phi_k(t+T)\rangle = |\Phi_k(t)\rangle$.

4.2.1.2 Simplifying Assumptions

For practical applications (4.13) can often be simplified as follows: (1) If the molecule has no permanent dipole, $\mathbf{g}_{\mathrm{XX}} = \mathbf{g}_{\mathrm{AA}} = \mathbf{0}$. (2) If the intrinsic nonadiabatic couplings can be neglected, $\boldsymbol{\lambda} = \mathbf{0}$. (3) Finally, if $\hbar\omega_1$ is resonant with the electronic excitation between the states X and A, nonresonant light-matter coupling terms can be neglected up to moderate field strengths. This leaves only those $\mathbf{g}_{\alpha\beta}$ matrices nonzero which connect $(\mathbf{H}_{\mathrm{X}} + n\hbar\omega_1\mathbf{I})$-type elements with $(\mathbf{H}_{\mathrm{A}} + (n-1)\hbar\omega_1\mathbf{I})$-type elements. The above three simplifications lead to a block-diagonal $\mathbf{H}_{\mathrm{F}}$, with each two-by-two block being essentially identical, differing only in the value of n in the terms $n\hbar\omega_1\mathbf{I}$ and $(n-1)\hbar\omega_1\mathbf{I}$. The block labeled with the Fourier index n reads

$$\mathbf{H}_{\mathrm{F}}^{2\times 2}(n) = \begin{bmatrix} \mathbf{H}_{\mathrm{X}} + n\hbar\omega_1 & \mathbf{g}_{\mathrm{XA}} \\ \mathbf{g}_{\mathrm{XA}}^{\dagger} & \mathbf{H}_{\mathrm{A}} + (n-1)\hbar\omega_1\mathbf{I} \end{bmatrix}. \tag{4.19}$$

Therefore, instead of solving the general problem presented in (4.11), it becomes sufficient to solve the eigenvalue problem for $\mathbf{H}_{\mathrm{F}}^{2\times 2}(n)$ in order to obtain the light-dressed states and the corresponding quasienergies. Therefore, the above simplifications lead to light-dressed states of the form

$$|\Phi_k(n)\rangle = \sum_{v,J} C_{\mathrm{X}vJ}^{(k)} |\mathrm{X}vJ\rangle|n\rangle + \sum_{v,J} C_{\mathrm{A}vJ}^{(k)} |\mathrm{A}vJ\rangle|n-1\rangle. \tag{4.20}$$

4.2.2 *Temporal Evolution of a Light-Dressed System*

In the representation of (4.12), the $\mathbf{H}_{\mathrm{F}}$ matrix corresponding to the Floquet Hamiltonian and the $C_{n,\alpha vJ}^{(k)}$ expansion coefficients of the Floquet states are both independent of time. Based on this representation, as well as (4.4) and (4.6), the temporal evolution of a light-dressed system can be expressed as [14]

$$\boldsymbol{\Psi}(t) = \sum_k c_k e^{-\frac{i}{\hbar}\mathbf{H}_{\mathrm{F}}t}\boldsymbol{\Phi}_k = e^{-\frac{i}{\hbar}\mathbf{H}_{\mathrm{F}}t}\sum_k c_k\boldsymbol{\Phi}_k = e^{-\frac{i}{\hbar}\mathbf{H}_{\mathrm{F}}t}\boldsymbol{\Psi}(t=0), \tag{4.21}$$

which is formally equivalent to the temporal evolution of a system with a time-independent Hamiltonian.

In a physical scenario when the dressing field amplitude changes slowly with time, those matrix elements of $\mathbf{H}_{\mathrm{F}}$ which represent light-matter couplings change also slowly with time. For a dressing field which is turned on much slower than the characteristic timescales of the field-free system, i.e., adiabatically, (4.21) suggests

that the well-known adiabatic theorem could be used to predict the temporal changes in $\mathbf{\Psi}(t)$. Therefore, in the limit of the dressing light intensity going to zero ($\mathbf{g}_{\mathrm{XA}} \rightarrow 0$), the field-free eigenstates are eigenstates of $\mathbf{H}_{\mathrm{F}}$ as well, and the adiabatic turn-on of the dressing field will convert an initial field-free eigenstate into a single light-dressed state. This means that light-dressed states and field-free states can be correlated in a one-to-one fashion. However, it is important to mention that the one-to-one correlation is not possible if ω_1 is in exact resonance with an allowed transition, because in that case the field-free eigenstates are not eigenstates of $\mathbf{H}_{\mathrm{F}}$ but are linear combinations of $\mathbf{H}_{\mathrm{F}}$ eigenstates even for infinitesimal light-matter coupling strengths. Further information on the temporal evolution of light-dressed states in the Floquet formalism and its possible utilization can be found, for example, in Refs. [35–38].

4.2.3 Transitions Between Light-Dressed States

Once the light-dressed states are determined, one can compute the transition probabilities between the different light-dressed states induced by the weak probe pulse. Following the standard approach of molecular spectroscopy [39], we use first-order time-dependent perturbation theory (TDPT) to derive the relevant equations.

4.2.3.1 General Considerations

Let us assume that the molecule interacts with two periodic electric fields, oscillating with frequencies ω_1 and ω_2. The full Hamiltonian then reads as

$$\hat{H}(t) = \hat{H}_{\mathrm{mol}} + \hat{W}_1(t) + \hat{W}_2(t), \tag{4.22}$$

where $\hat{W}_1(t)$ and $\hat{W}_2(t)$ represent the interaction between the molecule and the two fields. In the dipole approximation

$$\begin{aligned} \hat{W}_1(t) &= -\mathbf{E}_1 \hat{\boldsymbol{\mu}} \cos(\omega_1 t + \phi) \\ \hat{W}_2(t) &= -\mathbf{E}_2 \hat{\boldsymbol{\mu}} \cos(\omega_2 t). \end{aligned} \tag{4.23}$$

$\hat{W}_1(t)$ generates the light-dressed states, while $\hat{W}_2(t)$ represents the interaction with a weak probe pulse used to record the spectrum of the light-dressed molecule. The formation of light-dressed states by $\hat{W}_1(t)$ is described within the Floquet approach, as overviewed in Sect. 4.2.1. For computing the $\hat{W}_2(t)$-induced transition amplitudes between individual light-dressed states or between the superpositions of light-dressed states, first-order time-dependent perturbation theory is used. To derive our working equations, we start with the TDSE containing the interaction with both the dressing and the probe fields,

$$i\hbar\partial_t|\Psi(t)\rangle = (\hat{H}_{\rm mol} + \hat{W}_1(t) + \hat{W}_2(t))|\Psi(t)\rangle = (\hat{H}_{\rm d}(t) + \hat{W}_2(t))|\Psi(t)\rangle. \quad (4.24)$$

Equation (4.24) is transformed to the interaction picture using the transformation

$$|\Psi_{\rm I}(t)\rangle = e^{\frac{i}{\hbar}\int_{t_0}^{t}\hat{H}_{\rm d}(t')dt'}|\Psi(t)\rangle, \quad (4.25)$$

which leads to

$$i\hbar\partial_t|\Psi_{\rm I}(t)\rangle = \hat{W}_{2\rm I}(t)|\Psi_{\rm I}(t)\rangle, \quad (4.26)$$

where $\hat{W}_{2\rm I}(t) = e^{\frac{i}{\hbar}\int_{t_0}^{t}\hat{H}_{\rm d}(t')dt'}\hat{W}_2(t)e^{-\frac{i}{\hbar}\int_{t_0}^{t}\hat{H}_{\rm d}(t')dt'}$. Following the usual TDPT procedure of integrating (4.26) from t_0 to t and applying successive approximations to express $|\Psi_{\rm I}(t)\rangle$ gives

$$|\Psi_{\rm I}(t)\rangle = \hat{U}(t,t_0)|\Psi_{\rm I}(t_0)\rangle \quad (4.27)$$

with

$$\hat{U}(t,t_0) = \hat{I} + \frac{1}{i\hbar}\int_{t_0}^{t}\hat{W}_{2\rm I}(t')dt' + \frac{1}{(i\hbar)^2}\int_{t_0}^{t}\hat{W}_{2\rm I}(t')\int_{t_0}^{t'}\hat{W}_{2\rm I}(t'')dt''dt' + \cdots. \quad (4.28)$$

Taking the first two terms of the propagator in (4.28) leads to

$$|\Psi_{\rm I}(t)\rangle = |\Psi_{\rm I}(t_0)\rangle + \frac{1}{i\hbar}\int_{t_0}^{t}\hat{W}_{2\rm I}(t')dt'|\Psi_{\rm I}(t_0)\rangle. \quad (4.29)$$

The amplitude of the transition to a final state $|\Psi_{\rm I}^{(\rm F)}\rangle$ at time t is thus

$$\langle\Psi_{\rm I}^{(\rm F)}|\Psi_{\rm I}(t)\rangle = \langle\Psi_{\rm I}^{(\rm F)}|\Psi_{\rm I}(t_0)\rangle + \frac{1}{i\hbar}\int_{t_0}^{t}\langle\Psi_{\rm I}^{(\rm F)}|\hat{W}_{2\rm I}(t')|\Psi_{\rm I}(t_0)\rangle dt'. \quad (4.30)$$

By expanding $|\Psi_{\rm I}^{(\rm F)}\rangle$ and $|\Psi_{\rm I}(t_0)\rangle$ as a superposition of the $|\Phi_k(t_0)\rangle$ Floquet states,

$$|\Psi_{\rm I}^{(\rm F)}\rangle = \sum_l a_l e^{-\frac{i}{\hbar}\varepsilon_l t_0}|\Phi_l(t_0)\rangle \quad (4.31)$$

and

$$|\Psi_{\rm I}(t_0)\rangle = \sum_k b_k e^{-\frac{i}{\hbar}\varepsilon_k t_0}|\Phi_k(t_0)\rangle, \quad (4.32)$$

equation (4.30) gives

$$\langle\Psi_{\mathrm{I}}^{(\mathrm{F})}|\Psi_{\mathrm{I}}(t)\rangle = \sum_{l,k} a_l^* b_k e^{-\frac{i}{\hbar}(\varepsilon_k-\varepsilon_l)t_0}\langle\Phi_l(t_0)|\Phi_k(t_0)\rangle$$
$$+\frac{1}{i\hbar}\sum_{l,k} a_l^* b_k \int_{t_0}^{t} e^{-\frac{i}{\hbar}(\varepsilon_k-\varepsilon_l)t_0}\langle\Phi_l(t_0)|\hat{W}_{2\mathrm{I}}(t')|\Phi_k(t_0)\rangle dt'$$
$$= \sum_{l,k} a_l^* b_k e^{-\frac{i}{\hbar}(\varepsilon_k-\varepsilon_l)t_0}\langle\Phi_l(t_0)|\Phi_k(t_0)\rangle$$
$$+\frac{1}{i\hbar}\sum_{l,k} a_l^* b_k \int_{t_0}^{t} e^{-\frac{i}{\hbar}(\varepsilon_k-\varepsilon_l)t_0}\langle\Phi_l(t_0)|e^{\frac{i}{\hbar}\int_{t_0}^{t'}\hat{H}_{\mathrm{d}}(t'')dt''}\hat{W}_2(t')e^{-\frac{i}{\hbar}\int_{t_0}^{t'}\hat{H}_{\mathrm{d}}(t'')dt''}|\Phi_k(t_0)\rangle dt'. \quad (4.33)$$

Because $e^{-\frac{i}{\hbar}\varepsilon_k t}|\Phi_k(t)\rangle$ is a solution of the TDSE of (4.3), the effect of the $\hat{U}_{\mathrm{d}}(t', t_0) = e^{-\frac{i}{\hbar}\int_{t_0}^{t'}\hat{H}_{\mathrm{d}}(t'')dt''}$ operator, describing $\hat{H}_{\mathrm{d}}(t)$-governed time evolution from t_0 to t', can be evaluated as $\hat{U}_{\mathrm{d}}(t', t_0)(e^{-\frac{i}{\hbar}\varepsilon_k t_0}|\Phi_k(t_0)\rangle) = e^{-\frac{i}{\hbar}\varepsilon_k t'}|\Phi_k(t')\rangle$. Utilizing this expression, one obtains

$$\langle\Psi_{\mathrm{I}}^{(\mathrm{F})}|\Psi_{\mathrm{I}}(t)\rangle = \sum_{l,k} a_l^* b_k e^{-\frac{i}{\hbar}(\varepsilon_k-\varepsilon_l)t_0}\langle\Phi_l(t_0)|\Phi_k(t_0)\rangle$$
$$+\frac{1}{i\hbar}\sum_{l,k} a_l^* b_k \int_{t_0}^{t}\langle\Phi_l(t')|\hat{W}_2(t')|\Phi_k(t')\rangle e^{-\frac{i}{\hbar}(\varepsilon_k-\varepsilon_l)t'}dt'. \quad (4.34)$$

Finally, using the explicit form of $\hat{W}_2(t)$ given in (4.23) and expressing the periodic $|\Phi_k(t)\rangle$ functions under the integral with their Fourier series [see (4.7)], we obtain

$$\langle\Psi_{\mathrm{I}}^{(\mathrm{F})}|\Psi_{\mathrm{I}}(t)\rangle = \sum_{l,k} a_l^* b_k e^{-\frac{i}{\hbar}(\varepsilon_k-\varepsilon_l)t_0}\langle\Phi_l(t_0)|\Phi_k(t_0)\rangle$$
$$-\frac{1}{2i\hbar}\sum_{l,k} a_l^* b_k \sum_{n,m}\int_{t_0}^{t}\langle\varphi_{ln}|\mathbf{E}_2\hat{\boldsymbol{\mu}}|\varphi_{km}\rangle e^{-\frac{i}{\hbar}(\hbar\omega_1(n-m)+\varepsilon_k-\varepsilon_l\pm\hbar\omega_2)t'}dt'. \quad (4.35)$$

4.2.3.2 Simplifying Assumptions

For molecules with negligible intrinsic nonadiabatic couplings and no or negligibly small permanent dipole, such as the Na_2 molecule investigated below, the light-dressed states determined within a Floquet approach, in which nonresonant coupling terms with the dressing field are neglected [see (4.19)], (4.7) can be written as

$$|\Phi_k(t)\rangle = \sum_n (|\alpha_{kn}\rangle + |\beta_{k(n-1)}\rangle e^{-i\omega_1 t})e^{in\omega_1 t}, \quad (4.36)$$

where $|\alpha_{kn}\rangle$ and $|\beta_{k(n-1)}\rangle$ represent the two manifolds of rovibronic states with Fourier indices n and $n-1$, respectively. If the nonresonant coupling terms are neglected in the Floquet approach, the Floquet Hamiltonian becomes block diagonal [see (4.19)], $|\alpha_{kn}\rangle$ and $|\beta_{k(n-1)}\rangle$ become the same for all n, and (4.36) is simplified to

$$|\Phi_k(t)\rangle = (|\alpha_k\rangle + |\beta_k\rangle e^{-i\omega_1 t})e^{in\omega_1 t}. \tag{4.37}$$

In (4.37), $|\Phi_k(t)\rangle$ is a Floquet state obtained from the nth two-by-two block of the Floquet Hamiltonian, and the quasienergy associated with $|\Phi_k(t)\rangle$ may be written as $\varepsilon_k + \hbar n\omega_1$. As explained under (4.6), if the quasienergy is shifted by $-\hbar n\omega_1$ and the Floquet state is multiplied by $e^{-in\omega_1 t}$, one obtains an equivalent physical state. Therefore, (4.37) can be rewritten as

$$|\Phi_k(t)\rangle = |\alpha_k\rangle + |\beta_k\rangle e^{-i\omega_1 t}, \tag{4.38}$$

with the corresponding quasienergy ε_k. Using (4.38) instead of (4.7) leads to a simplified version of (4.35),

$$\begin{aligned}\langle \Psi_{\mathrm{I}}^{(\mathrm{F})}|\Psi_{\mathrm{I}}(t)\rangle = &\sum_{l,k} a_l^* b_k e^{-\frac{i}{\hbar}(\varepsilon_k-\varepsilon_l)t_0}\langle\Phi_l(t_0)|\Phi_k(t_0)\rangle \\ &-\frac{1}{2i\hbar}\sum_{l,k} a_l^* b_k \int_{t_0}^{t}\langle\beta_l|\mathbf{E}_2\hat{\boldsymbol{\mu}}|\alpha_k\rangle e^{-\frac{i}{\hbar}(\varepsilon_k-\varepsilon_l-\hbar\omega_1\pm\hbar\omega_2)t'}dt' \\ &-\frac{1}{2i\hbar}\sum_{l,k} a_l^* b_k \int_{t_0}^{t}\langle\alpha_l|\mathbf{E}_2\hat{\boldsymbol{\mu}}|\beta_k\rangle e^{-\frac{i}{\hbar}(\varepsilon_k-\varepsilon_l+\hbar\omega_1\pm\hbar\omega_2)t'}dt', \end{aligned} \tag{4.39}$$

where we use the fact that $\langle\alpha_l|\mathbf{E}_2\hat{\boldsymbol{\mu}}|\alpha_k\rangle = \langle\beta_l|\mathbf{E}_2\hat{\boldsymbol{\mu}}|\beta_k\rangle = 0$ for a molecule with no permanent dipole. By following the standard TDPT procedure, and assuming that the initial and final states of the transition in (4.39) are the kth and lth light-dressed states, the $T_{l\leftarrow k}$ transition amplitude becomes

$$\begin{aligned} T_{l\leftarrow k} \propto &\sum_{v,J}\sum_{v',J'} C^{(l)*}_{\mathrm{A}v'J'} C^{(k)}_{\mathrm{X}vJ}\langle \mathrm{A}v'J'|\mathbf{E}_2\hat{\boldsymbol{\mu}}|\mathrm{X}vJ\rangle\delta(\varepsilon_k-\varepsilon_l-\hbar\omega_1\pm\hbar\omega_2) \\ &+\sum_{v,J}\sum_{v',J'} C^{(l)*}_{\mathrm{X}v'J'} C^{(k)}_{\mathrm{A}vJ}\langle \mathrm{X}v'J'|\mathbf{E}_2\hat{\boldsymbol{\mu}}|\mathrm{A}vJ\rangle\delta(\varepsilon_k-\varepsilon_l+\hbar\omega_1\pm\hbar\omega_2). \end{aligned} \tag{4.40}$$

Based on the arguments of the delta functions in (4.40), the first term can be interpreted as a transition between the light-dressed states having quasienergies ε_k and $\varepsilon_l + \hbar\omega_1$, that is, in the notation of (4.20), a transition between $|\Phi_k(n)\rangle$ and $|\Phi_l(n')\rangle$ with $n = n' - 1$. Similarly, the second term in (4.40) can be interpreted as a transition between $|\Phi_k(n)\rangle$ and $|\Phi_l(n')\rangle$ with $n = n' + 1$.

4.3 Computational Details

To illustrate the numerical results one can derive *via* the theory introduced in Sect. 4.2, we investigate the Na_2 molecule. In the simulations we consider the $X\,^1\Sigma_g^+$ ground state and the first excited $A\,^1\Sigma_u^+$ electronic state of Na_2, which we represent with the potential energy curves (PEC) on [40]. The transition dipole function between these two states is taken from [41]. The field-free rovibrational wave functions of Na_2 on the $V_X(R)$ and $V_A(R)$ PECs are computed using 200 spherical-DVR basis functions [42] with the related grid points placed in the internuclear coordinate range (0, 10) bohr. All rovibrational eigenstates with $J < 16$ and whose energy does not exceed the zero-point energy of the respective PEC by more than $2000\,\mathrm{cm}^{-1}$ were included in the basis representing the Floquet Hamiltonian of (4.19), which was then diagonalized to obtain the light-dressed states.

In all computations the polarization vector of the pump pulse was assumed to be parallel to the polarization vector of the probe pulse. Therefore, the projection of the total angular momentum onto this axis is a conserved quantity in our simulations.

When investigating the effect of the turn-on time of the dressing field (see Sect. 4.4.5), the TDSE was solved using the simple formula $\mathbf{\Psi}(t + dt) = e^{-(i/\hbar)\mathbf{H}(t)dt}\mathbf{\Psi}(t)$. Due to the small size of $\mathbf{H}(t)$ (few thousand by few thousand) the exponential function could be constructed by diagonalizing $\mathbf{H}(t)$ at each time step.

4.4 Results and Discussion

4.4.1 Interpretation of the Light-Dressed Spectrum

Before the light-dressed spectra are investigated in detail, it is worth considering their expected structure qualitatively. Naturally, the light-dressed spectrum strongly depends on the molecule investigated and the properties of the dressing field. For Na_2 the rotational, vibrational, and electronic transition wavenumbers considered in this work are of the orders of 1,100, and 15,000 cm^{-1}, respectively. Figure 4.1 depicts the landscape of light-dressed PECs for the Na_2 molecule dressed by light whose wavelength is $\lambda = 662$ nm. As can be seen in Fig. 4.1, the manifolds of light-dressed states labeled by n are well separated from each other. Based on (4.40), arrows are drawn to indicate the physical origin of possible absorption and stimulated emission processes induced by the probe pulse. Absorption is described by the first term in (4.40), in which the initial light-dressed state contributes through its X ground electronic state component and the final state contributes through its A excited electronic state component. On the other hand, stimulated emission originates from the second term in (4.40), in which the initial light-dressed state contributes through its A excited electronic state component and the final state contributes through its X ground electronic state component.

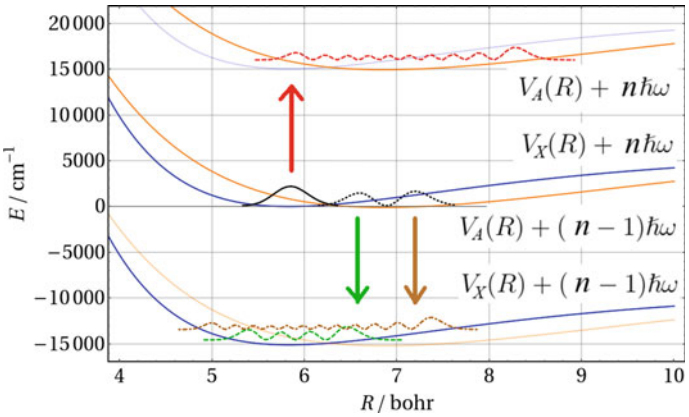

Fig. 4.1 Light-dressed diabatic potential-energy curves (PECs) of Na_2 obtained with a dressing-light whose wavelength is $\lambda = 662$ nm. The energy scale stands for the quasienergy of Floquet theory [33]. Probability densities from the vibrational wave functions are drawn for the $|\mathrm{X}\ 0\ 0\rangle|n\rangle$ (continous black line on the $V_\mathrm{X}(R) + n\hbar\omega_1$ PEC), $|\mathrm{X}\ 3\ 0\rangle|n-1\rangle$ (green dashed line on the $V_\mathrm{X}(R) + (n-1)\hbar\omega_1$ PEC), $|\mathrm{X}\ 11\ 0\rangle|n-1\rangle$ (brown dashed line on the $V_\mathrm{X}(R) + (n-1)\hbar\omega_1$ PEC), $|\mathrm{A}\ 1\ 1\rangle|n-1\rangle$ (black dotted line on the $V_\mathrm{A}(R) + (n-1)\hbar\omega_1$ PEC), and $|\mathrm{A}\ 9\ 1\rangle|n\rangle$ (red dashed line on the $V_\mathrm{A}(R) + n\hbar\omega_1$ PEC) states. Up- and downward vertical arrows represent absorption and stimulated emission, respectively. The two product states with the largest contribution to the light-dressed state correlating to $|\mathrm{X}\ 0\ 0\rangle$ at $|E_1| \to 0$ are $|\mathrm{X}\ 0\ 0\rangle|n\rangle$ and $|\mathrm{A}\ 1\ 1\rangle|n-1\rangle$

4.4.2 Intensity Dependence of the Light-Dressed Spectrum

Figure 4.2 shows absorption and stimulated emission spectra of Na_2 at 0 K, when dressed by light fields of different intensity and a wavelength of 662 nm.

As seen in Fig. 4.2, the height of the envelopes of both the absorption and the stimulated emission spectra increase with increasing dressing-field intensity, while the stimulated emission peaks disappear at the limit of zero dressing-field intensity. We point out here that the light-dressed states and the corresponding light-dressed spectra change when the dressing field wavelength is changed. Therefore, if dressing light wavelengths different from 662 nm are used, the height of the envelope of the absorption spectrum might decrease or even fluctuate with increasing dressing light intensity.

Inspecting the individual transition lines reveals that the light-dressing process leads to the splitting of field-free absorption peaks as well as the appearance of new peaks, as shown in the upper and lower panels of Fig. 4.3, respectively. Assignment and understanding of the physical origin of the transition peaks of the light-dressed spectrum can be based on the selection rules governing transitions between field-free states and on the fact that the light-dressed states can be described as a superposition of field-free states.

For example, the upper panel of Fig. 4.3 shows the progression of three peaks, corresponding to the transitions from the initial state (the light-dressed state corre-

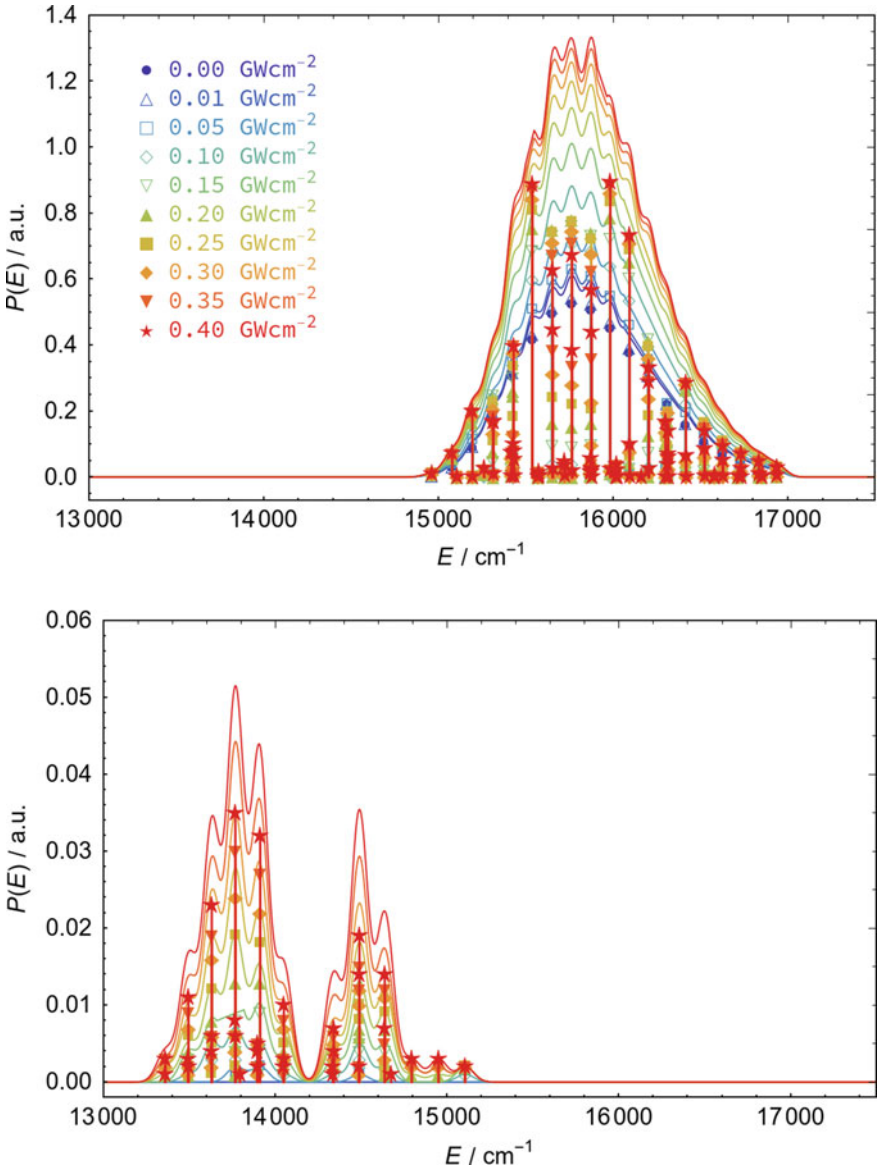

Fig. 4.2 Absorption (upper panel) and stimulated emission (lower panel) spectra of Na_2 dressed with 662 nm wavelength laser lights of different intensity, at 0 K. The stick spectra were computed using (4.40) and show transitions from the field-dressed state, which correlates to the $|X\ 0\ 0\rangle$ rovibronic ground state in the limit of the dressing field intensity going to zero. The envelopes shown are obtained by taking the convolution of the stick spectra with a Gaussian function having a standard deviation of 50 cm^{-1}

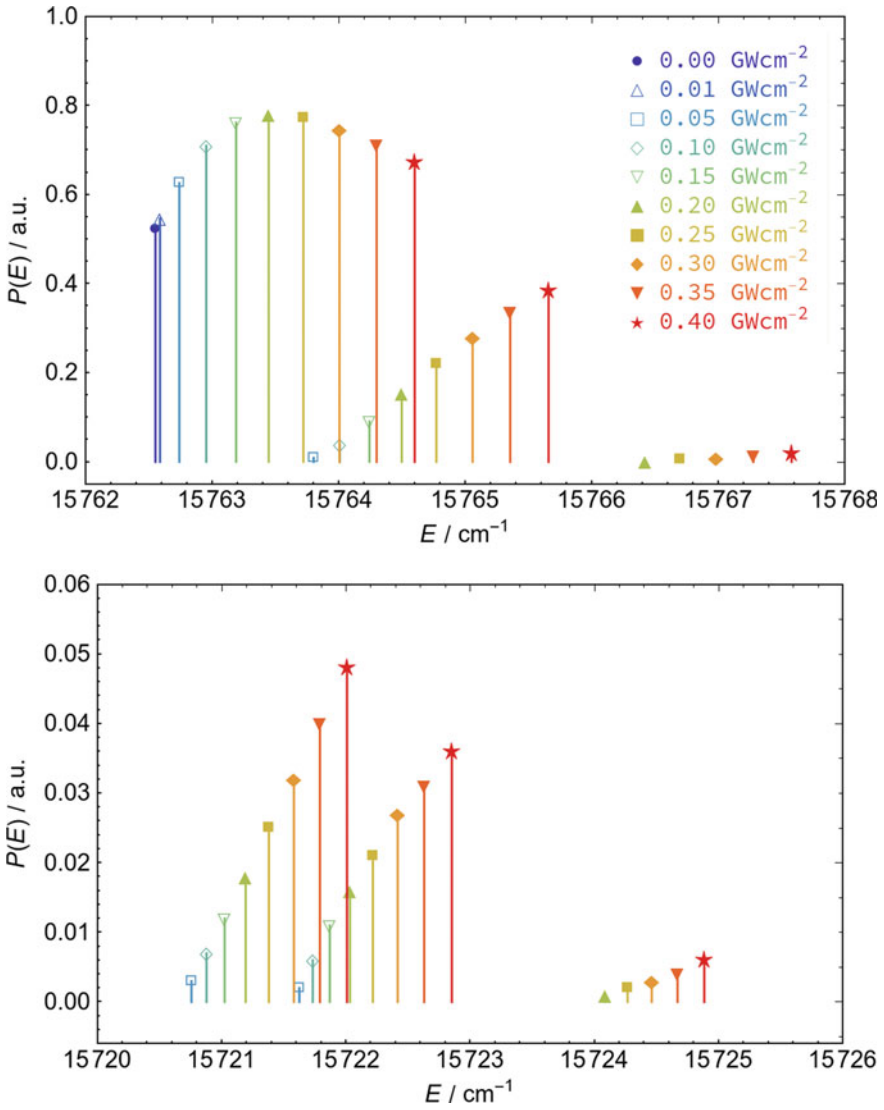

Fig. 4.3 Progression of selected light-dressed absorption peaks of Na_2 dressed with a 662 nm wavelength laser light at 0 K. The upper panel shows peaks originating from the field-free transition $|X\ 0\ 0\rangle \rightarrow |A\ 7\ 1\rangle$, while the lower panel shows peaks which have no field-free counterpart

lating to the field-free ground state) composed primarily of the $|X\ 0\ 0\rangle$ state with smaller contributions from the $|X\ 0\ 2\rangle$ and $|A\ 1\ 1\rangle$ states to the light-dressed states composed primarily of the $|A\ 7\ 1\rangle$, $|A\ 7\ 3\rangle$, and $|A\ 7\ 5\rangle$ states, with $|X\ v\ J\rangle$-type states (J even) contributing as well. These transitions can be interpreted as those originating from the field-free transition $|X\ 0\ 0\rangle \rightarrow |A\ 7\ 1\rangle$, which is split due to the

mixing of field-free states through the light-matter coupling with the dressing field. Such type of peak splittings are similar to the well-known *Autler–Townes effect* [24], which is a useful tool in spectroscopy, see, for example [25–27]. The upper panel of Fig. 4.3 not only demonstrates splitting of the peak, in which the sum of individual peak intensities remain unchanged, but exhibits an overall increase in the peak intensities when the strength of the dressing field is increased. In spectroscopy the changes in transition peak intensities resulting from couplings between eigenstates of a zeroth-order Hamiltonian is called *intensity borrowing* [39].

The lower panel of Fig. 4.3 shows the progression of three peaks, which appear as new peaks rather than arising from the splitting of a field-free peak. These transitions occur between the initial state (light-dressed state correlating to the field-free ground state) composed primarily of $|\mathrm{X}\,0\,0\rangle$ with smaller contributions from $|\mathrm{X}\,0\,2\rangle$ and $|\mathrm{A}\,1\,1\rangle$ and the light-dressed states composed primarily of the $|\mathrm{X}\,4\,0\rangle$, $|\mathrm{X}\,4\,2\rangle$, and $|\mathrm{X}\,4\,4\rangle$ states. Such transitions are forbidden in the limit of zero dressing-light intensity; however, they become visible as the light-matter coupling with the dressing field mixes the $|\mathrm{X}\,4\,J\rangle$ states (J even) with $|\mathrm{A}\ v\ 1\rangle$-type states, to which $|\mathrm{X}\,0\,0\rangle$ has non-zero transition probability. The appearance of transition peaks as a result of such a mixing can be understood as an intensity-borrowing effect.

As to the stimulated emission peaks shown in the lower panel of Fig. 4.2, they represent transitions from the initial state to the light-dressed states composed primarily of the vibrationally highly excited $|\mathrm{X}\,v\,0\rangle$- and $|\mathrm{X}\,v\,2\rangle$-type states, with $|\mathrm{A}\,v'\,J\rangle$-type states ($J$ odd) also giving a small contribution.

4.4.2.1 Predicting Field-Free Properties Using Extrapolation

Although light-dressed spectroscopy might yield transition peaks forbidden in the field-free case, the transition wavenumbers between light-dressed states are in general different from the transition wavenumbers between field-free states. If one is interested in obtaining field-free transition wavenumbers, one can record the light-dressed spectrum at several dressing-field intensities and extrapolate to the zero intensity limit. Such a procedure is of course most valuable when the transition is forbidden in the field-free case.

As an example, we examine the stimulated emission peak at around $13{,}770\,\mathrm{cm}^{-1}$ (see Fig. 4.4). The emission peak around $13{,}770\,\mathrm{cm}^{-1}$ represents a transition in which the initial state is composed primarily of the $|\mathrm{X}\,0\,0\rangle$ ground state and has small contributions from the $|\mathrm{X}\,0\,2\rangle$ and $|\mathrm{A}\,1\,1\rangle$ states, and in which the final state is composed primarily of $|\mathrm{X}\,9\,2\rangle$, with $|\mathrm{X}\,9\,0\rangle$ and $|\mathrm{A}\,13\,1\rangle$ giving a small contribution, as well. In the limit of zero dressing-light intensity, the initial and final states correlate to $|\mathrm{X}\,0\,0\rangle$ and $|\mathrm{X}\,9\,2\rangle$, respectively. Transitions between these two field-free states is forbidden; nonetheless, their accurate transition wavenumber can be obtained by extrapolating the light-dressed transition wavenumber to the limit of zero dressing light intensity. As expected and seen in Fig. 4.4, linear extrapolation might be pursued if data points at low dressing-light intensities are used. On the other hand, by increasing the dressing-light intensity above a certain level, the relation between intensity and tran-

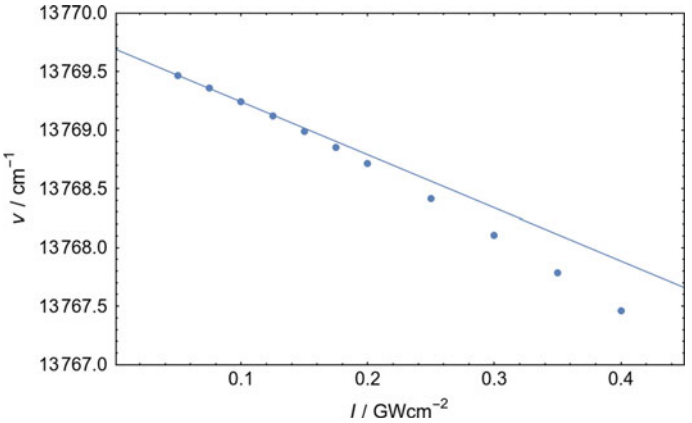

Fig. 4.4 Position of the stimulated emission peak near 13,770 cm^{-1} as a function of dressing light intensity for a $\lambda = 662$ nm laser light. The straight line plotted was obtained by a linear fit to the first four data points

sition wavenumber becomes nonlinear. As seen in Fig. 4.4, the value of the transition wavenumber extrapolated to zero intensity is 13,769.7 cm^{-1}. Considering that the $|X\,0\,0\rangle$ and $|X\,9\,2\rangle$ states involved in this transition belong to the n and $n-1$ Fourier manifolds (see Fig. 4.1), the transition wavenumber between $|X\,0\,0\rangle$ and $|X\,9\,2\rangle$ can be calculated to be 1336.0 $cm^{-1} = (15,105.7 - 13,769.7)$ cm^{-1}, where 15,105.7 cm^{-1} is the photon energy of the dressing light. The numerical value for the transition wavenumber, obtained as the difference between the computed field-free eigenenergies, is 1336.1 $cm^{-1} = (1415.4 - 79.3)$ cm^{-1}, where 1415.4 and 79.3 cm^{-1} are the computed energies of the $|X\ 9\ 2\rangle$ and $|X\,0\,0\rangle$ states, respectively. Thus, this extrapolation technique works well.

4.4.3 Frequency Dependence of the Light-Dressed Spectrum

Figure 4.5 shows the light-dressed absorption and stimulated emission spectrum of Na_2 dressed by a light field whose intensity is $I = 10^8$ $W\,cm^{-2}$ at different wavelengths. As can be seen in Fig. 4.5, both the absorption and the stimulated emission spectra vary largely depending on the wavelength of the dressing light. This is the expected behavior because the contribution of different field-free states in the light-dressed states also vary depending on the dressing-light wavelength, leading to varying transition probabilities. Therefore, by changing the dressing-light wavelength, one can influence which transitions appear in the light-dressed spectrum.

Interestingly, the magnitudes of the Franck–Condon overlaps between the vibrational states of the X and A electronic states of Na_2 are reflected in the stimulated emission spectrum, i.e., the number of vertical nodes in the stimulated emission spec-

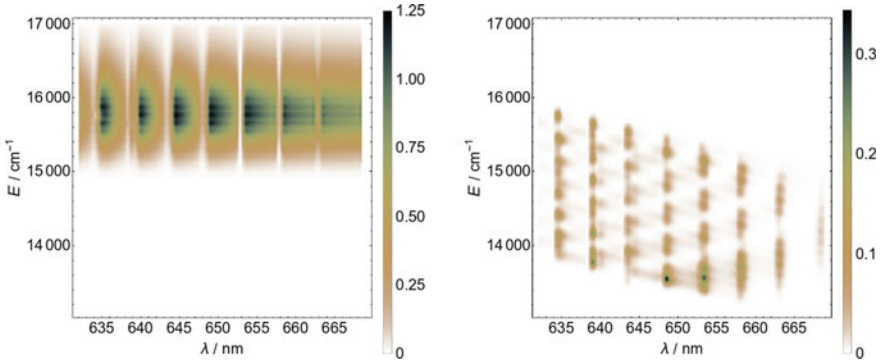

Fig. 4.5 Absorption (left panel) and stimulated emission (right panel) 0 K spectra of Na_2 dressed with an $I = 10^8$ W cm^{-2} intensity laser light of different wavelengths

trum at the different dressing-light wavelengths can reveal which v value of the $|\mathrm{A}\ v\ J\rangle$-type states contributes most to the initial light-dressed state. For example, using dressing light at 662 nm leads to emission lines whose transition amplitude primarily originate from $|\mathrm{A}\ 1\ J\rangle \rightarrow |\mathrm{X}\ v\ J \pm 1\rangle$-type transitions, while using a dressing light with 657 nm leads to emission lines whose transition amplitudes primarily originate from $|\mathrm{A}\ 2\ J\rangle \rightarrow |\mathrm{X}\ v\ J \pm 1\rangle$-type transitions.

4.4.4 Light-Dressed Spectra at Finite Temperatures

In the preceding sections it was assumed that the initial light-dressed state correlates to the field-free rovibronic ground state of Na_2, that is, the light-dressed spectra shown are those at $T = 0$ K. The physical picture behind this assumption is that initially the field-free molecules are all in their ground state and these are transformed into dressed states with the adiabatic turn-on of the dressing field. In a realistic experiment at a finite temperature, however, the molecules are not necessarily in their ground state, and thermal averaging of the computed spectrum needs to be carried out. Because thermal equilibrium is assumed prior to the light-dressing process, the thermal averaging can be done by weighting transitions with the Boltzmann weights of the field-free states correlating to the respective initial light-dressed states. That is, transitions from each $|\Phi_i\rangle$ light-dressed state are included in the computed spectrum, and all transitions from a given $|\Phi_i\rangle$ light-dressed state are weighted by

$$\frac{e^{-E_i^{\mathrm{FF}}/kT}}{Q(T)}, \tag{4.41}$$

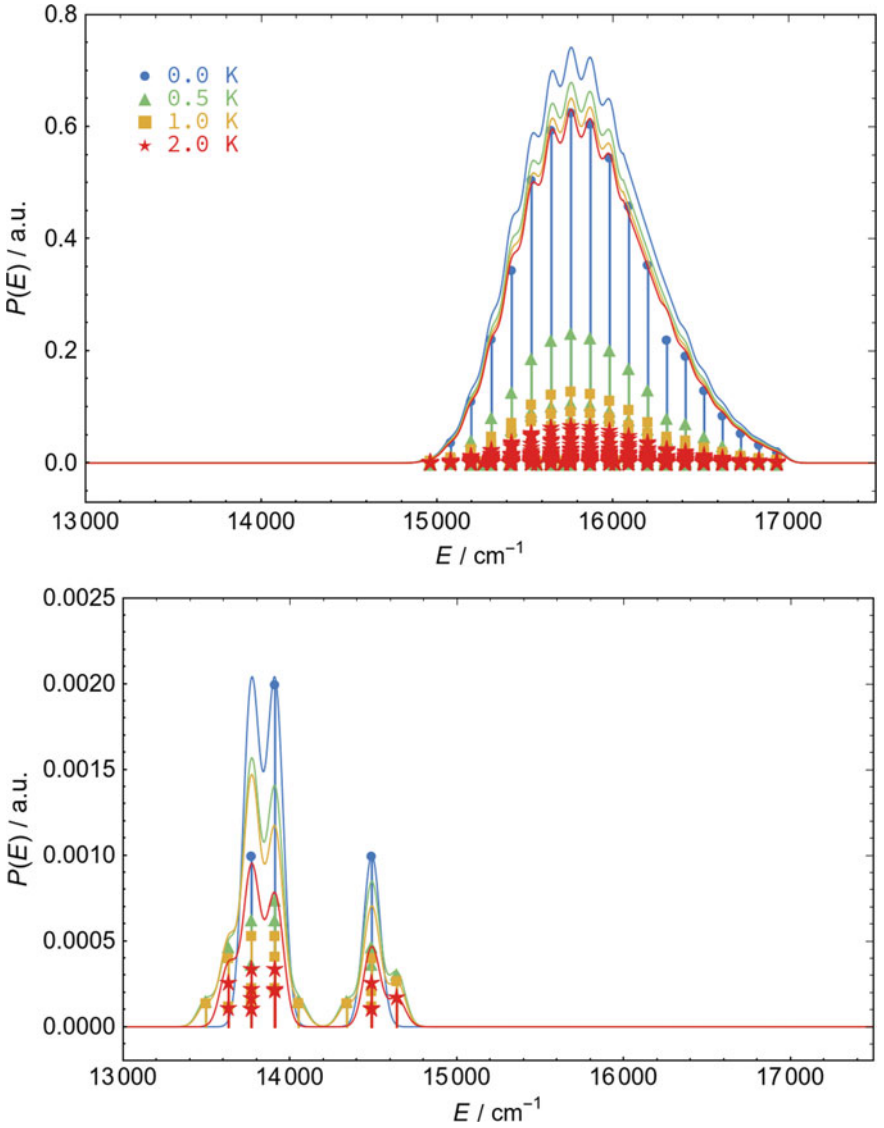

Fig. 4.6 Light-dressed absorption (upper panel) and stimulated emission (lower panel) spectra of Na_2 obtained at different temperatures with a dressing light whose wavelength and intensity are 662 nm and 5×10^7 Wcm^{-2}, respectively

where $Q(T) = \sum_i e^{-E_i^{\mathrm{FF}}/kT}$ is the rovibronic partition function of the field-free molecule, and E_i^{FF} is the energy of the field-free rovibronic state to which $|\Phi_i\rangle$ correlates in the limit of the dressing light intensity going to zero.

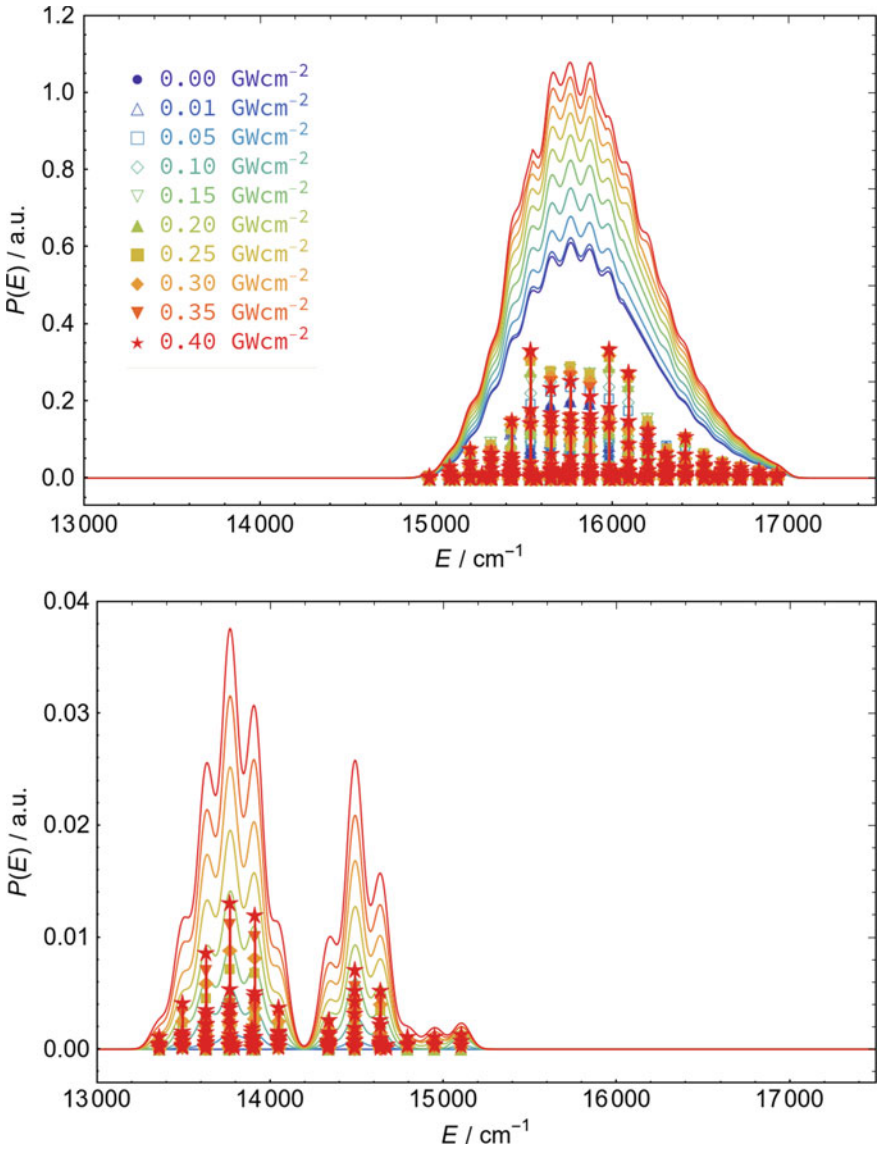

Fig. 4.7 Light-dressed absorption (upper panel) and stimulated emission (lower panel) spectra of Na_2 obtained at 0.5 K with 662 nm wavelength dressing fields having different intensities

At finite temperatures an additional complication arises. Namely, one needs to take into account the field-free rotational states of a closed-shell diatomic molecule which are characterized not only by J but also by the m quantum number, which stands for the projection of the rotational angular momentum onto the chosen space-

fixed quantization axis. Since a linearly polarized dressing field (and the weak probe pulse with identical polarization) can not mix states with different m quantum numbers, one can restrict the simulation to the $m = 0$ manifold when $T = 0$ K. In the finite temperature calculations, one needs to determine the light-dressed states and corresponding transitions for the different m manifolds, and include them in the spectrum with appropriate weights given by (4.41).

Figure 4.6 shows the light-dressed spectra of Na_2 at different temperatures when Na_2 is dressed by a light field whose wavelength and intensity are 662 nm and 5×10^7 Wcm^{-2}, respectively. The upper panel of Fig. 4.6 demonstrates that the absorption peaks exhibit splittings and that the height of the split peaks decrease significantly when the temperature increases. This is because the low-lying rotational states are populated at finite temperatures. Nonetheless, the height of the spectrum envelope is much less sensitive to the temperature than the individual peak heights. The effects of a temperature increase appear more significantly in the stimulated emission spectrum than in the absorption spectrum, as shown in the lower panel of Fig. 4.6.

Figure 4.7 shows the dependence of the light-dressed spectra on the dressing light intensity at $T = 0.5$ K. In a similar manner as in Fig. 4.6, the intensities of the spectral peaks in Fig. 4.7 are more influenced by the increase of temperature than the entire spectral envelope.

4.4.5 *Effects of the Dressing-Field Turn-On Time on the Light-Dressed States*

Up to this point it was assumed that the dressing field is turned on adiabatically. As explained in Sect. 4.2.2, the result is that an initial field-free eigenstate is transformed into a single light-dressed state during the dressing process. If the dressing field is not turned on adiabatically, the generated light-dressed wave function becomes a superposition of light-dressed states, with the coefficients depending on the turn-on time [35, 38, 43, 44].

Figure 4.8 demonstrates the population of the different field-free eigenstates in the wave function for dressing-fields of different turn-on time (Γ) and intensity. The functional form of the dressing light was assumed to be $\boldsymbol{E}_1(t) = \boldsymbol{0}$ for $t < 0$, $\boldsymbol{E}_1(t) = \boldsymbol{E}_{\max}\sin(\hbar\omega_1 t)\sin^2(\pi t/\Gamma)$ for $0 < t < \Gamma/2$, and $\boldsymbol{E}_1(t) = \boldsymbol{E}_{\max}$ for $\Gamma/2 < t$. The populations shown in Fig. 4.8 were computed for $t = \Gamma/2$ by solving the TDSE directly.

Based on the $|\mathrm{X}\ 0\ 0\rangle \leftrightarrow |\mathrm{X}\ 0\ 1\rangle$ transition of Na_2, the characteristic timescale of molecular rotations is around 100 ps. Panels (b) and (c) of Fig. 4.8 demonstrate that when the turn-on time is shorter than this characteristic timescale, the degree of rotational excitation is reduced. In fact, in the excited electronic state the rotational excitation is limited to that required by the optical selection rules ($\Delta J = \pm 1$). Panels (b) and (c) of Fig. 4.8 also demonstrate that as the turn-on time of the dressing light

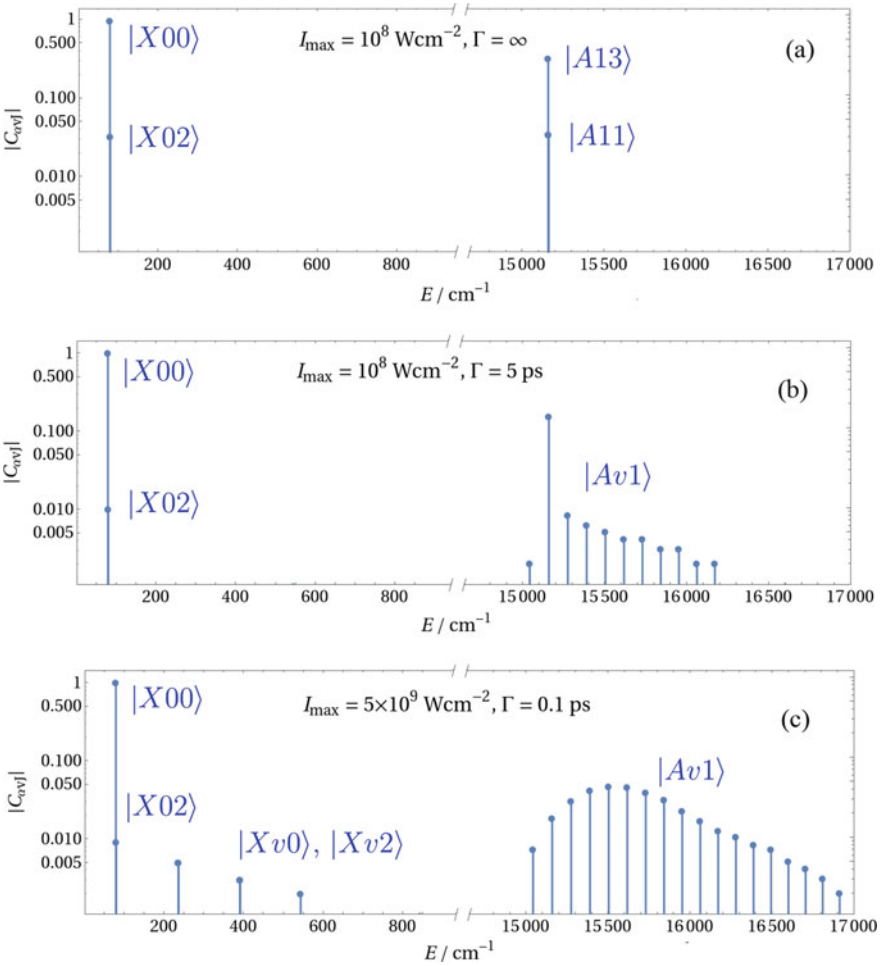

Fig. 4.8 Population of the different field-free eigenstates in the wave function for $\lambda = 663$ nm wavelength dressing-fields of different turn-on time and intensity

becomes shorter, its spectral width expands, giving rise to significant populations in $|\mathrm{A}\ v\ 1\rangle$-type field-free eigenstates in a wider energy range.

After the dressing field reaches its peak intensity at $t = \Gamma/2$ the wave function can be expanded as a superposition of the light-dressed states and the light-dressed spectrum can be calculated according to (4.35). If the probe pulse is long enough so that the interferences in the transition probability are averaged out, the light-dressed spectrum can be generated as a simple weighted sum of the spectra of individual light-dressed states.

In summary, by changing the turn-on time of the dressing field, the initial wave function can be manipulated, and in such a way the transition peaks observed in the light-dressed spectrum can be influenced or controlled. However, this might significantly complicate the interpretation of the spectrum.

4.5 Summary and Conclusions

We have presented a theoretical method to compute light-dressed spectra of molecules dressed by medium-intensity laser fields ($I = 10^7 - 5 \times 10^9$ Wcm^{-2} in the numerical examples of this work). The approach is based on Floquet theory for deriving the light-dressed states, which are expanded using field-free molecular eigenstates. Once the light-dressed states are determined, the transition amplitudes induced between them by a weak probe pulse are computed utilizing first-order perturbation theory.

A numerical example is given for the homonuclear diatomic molecule Na_2, for which the general formulae can be simplified and the rovibronic light-dressed spectra can be interpreted straigthforwardly. The simulations indicate that the light dressing process leads to the splitting of field-free peaks as well as the appearance of new peaks, which correspond to transitions forbidden in the field-free case. Processes corresponding to the well-known *intensity borrowing* and *Autler–Townes* effects of molecular spectroscopy can also be observed.

Dependence of the light-dressed rovibronic spectrum of Na_2 on the dressing light intensity and the dressing light wavelength was investigated, as well. It was found that one can influence and control the peaks appearing in the light-dressed spectra by manipulating the intensity and the wavelength of the dressing light.

We tested how the transition wavenumber of a forbidden field-free transition could be determined by extrapolating light-dressed transition frequencies to the limit of zero dressing-light intensity. The extrapolation scheme seemed to produce excellent results.

Calculations assuming different initial temperatures of the molecular ensemble prior to the dressing process reveal that the envelopes of the field-dressed spectra are much less sensitive to the initial temperature than the individual spectral peaks, similar to the field-free case.

Finally, it was shown that the initial wave function of the light-dressed system can be modified significantly when the turn-on time of the dressing field is changed from the adiabatic limit to shorter times, likely to result in significant changes in the light-dressed spectrum, as well.

Acknowledgements This research was supported by the EU-funded Hungarian grant EFOP-3.6.2-16-2017-00005. The authors are grateful to NKFIH for support (Grant No. PD124623 and K119658).

References

1. F. Merkt, M. Quack, Molecular quantum mechanics and molecular spectra, molecular symmetry, and interaction of matter with radiation, in *Handbook of High-Resolution Spectroscopy*, ed. by M. Quack, F. Merkt (Wiley, Chichester, 2011)
2. T. Udem, R. Holzwarth, T.W. Hänsch, Optical frequency metrology. Nature **416**, 233–237 (2002)
3. S.A. Diddams, The evolving optical frequency comb. J. Opt. Soc. Am. B **27**, B51 (2010)
4. J.L. Hall, Nobel lecture: defining and measuring optical frequencies. Rev. Mod. Phys. **78**, 1279–1295 (2006)
5. T.W. Hänsch, Nobel lecture: passion for precision. Rev. Mod. Phys. **78**, 1297–1309 (2006)
6. T. Brabec, F. Krausz, Intense few-cycle laser fields: frontiers of nonlinear optics. Rev. Mod. Phys. **72**, 545–591 (2000)
7. F. Krausz, M. Ivanov, Attosecond physics. Rev. Mod. Phys. **81**, 163–234 (2009)
8. A. Palacios, F. Martín, The quantum chemistry of attosecond molecular science. WIREs Comp. Mol. Sci. 20, e1430 (2020)
9. A.H. Zewail, Femtochemistry: atomic-scale dynamics of the chemical bond. J. Phys. Chem. A **104**, 5660–5694 (2000)
10. M. Dantus, Coherent nonlinear spectroscopy: from femtosecond dynamics to control. Annu. Rev. Phys. Chem. **52**, 639–679 (2001)
11. S. Mukamel, Multidimensional femtosecond correlation spectroscopies of electronic and vibrational excitations. Annu. Rev. Phys. Chem. **51**, 691–729 (2000)
12. T. Ando, A. Iwasaki, K. Yamanouchi, Strong-field fourier transform vibrational spectroscopy of $D_2{}^+$ using few-cycle near-infrared laser pulses. Phys. Rev. Lett. **120**, 263002 (2018)
13. C. Cohen-Tannoudji, J. Dupont-Roc, G. Grynberg, *Atom-Photon Interactions: Basic Processes and Applications* (Wiley-VCH Verlag GmbH and Co, KGaA, 2004)
14. J.H. Shirley, Solution of the Schrödinger equation with a Hamiltonian periodic in time. Phys. Rev. **138**, B979–B987 (1965)
15. C. Wunderlich, E. Kobler, H. Figger, T.W. Hänsch, Light-induced molecular potentials. Phys. Rev. Lett. **78**, 2333–2336 (1997)
16. B.M. Garraway, K.-A. Suominen, Adiabatic passage by light-induced potentials in molecules. Phys. Rev. Lett. **80**, 932–935 (1998)
17. Y. Sato, H. Kono, S. Koseki, Y. Fujimura, Description of molecular dynamics in intense laser fields by the time-dependent adiabatic state approach: application to simultaneous two-bond dissociation of CO_2 and its control. J. Am. Chem. Soc. **125**(26), 8019–8031 (2003)
18. M.E. Corrales, J. González-Vázquez, G. Balerdi, I.R. Solá, R. de Nalda, L. Bañares, Control of ultrafast molecular photodissociation by laser-field-induced potentials. Nat. Chem. **6**, 785–790 (2014)
19. F. Kelkensberg, C. Lefebvre, W. Siu, O. Ghafur, T.T. Nguyen-Dang, O. Atabek, A. Keller, V. Serov, P. Johnsson, M. Swoboda, T. Remetter, A. L'Huillier, S. Zherebtsov, G. Sansone, E. Benedetti, F. Ferrari, M. Nisoli, F. Lépine, M.F. Kling, M.J.J. Vrakking, Molecular dissociative ionization and wave-packet dynamics studied using two-color XUV and IR pump-probe spectroscopy. Phys. Rev. Lett. **103**, 123005 (2009)
20. O. Atabek, R. Lefebvre, T. Nguyen-Dang, Unstable states in laser assisted and controlled molecular processes, in *Unstable States in the Continuous Spectra, Part I: Analysis, Concepts, Methods, and Results*, pp. 51–104, (Elsevier, Amsterdam, 2010)
21. E.E. Aubanel, J.-M. Gauthier, A.D. Bandrauk, Molecular stabilization and angular distribution in photodissociation of $H_2{}^+$ in intense laser fields. Phys. Rev. A **48**, 2145–2152 (1993)
22. A.D. Bandrauk, M.L. Sink, Photodissociation in intense laser fields: predissociation analogy. J. Chem. Phys. **74**, 1110–1117 (1981)
23. P.H. Bucksbaum, A. Zavriyev, H.G. Muller, D.W. Schumacher, Softening of the $H_2{}^+$ molecular bond in intense laser fields. Phys. Rev. Lett. **64**, 1883–1886 (1990)
24. S.H. Autler, C.H. Townes, Stark effect in rapidly varying fields. Phys. Rev. **100**, 703–722 (1955)

25. A. Sanli, X. Pan, S. Magnier, J. Huennekens, A.M. Lyyra, E.H. Ahmed, Measurement of the Na_2 $5^1\sigma_g^+ \rightarrow A^1\sigma_u^+$ and $6^1\sigma_g^+ \rightarrow A^1\sigma_u^+$ transition dipole moments using optical-optical double resonance and Autler-Townes spectroscopy. J. Chem. Phys. **147**(20), 204301 (2017)
26. E.H. Ahmed, J. Huennekens, T. Kirova, J. Qi, A.M. Lyyra, The Autler-Townes effect in molecules: observations, theory, and applications. Adv. At., Mol., Opt. Phys. **61**, 467–514 (2012)
27. C.Y. Lee, B.H. Pate, Dressed states of molecules and microwave-infrared double-resonance spectroscopic techniques employing an electric quadrupole focusing field. J. Chem. Phys. **107**(24), 10430–10439 (1997)
28. G.J. Halász, Á. Vibók, M. Šindelka, N. Moiseyev, L.S. Cederbaum, Conical intersections induced by light: Berry phase and wavepacket dynamics. J. Phys. B **44**(17), 175102 (2011)
29. G.J. Halász, M. Šindelka, N. Moiseyev, L.S. Cederbaum, Á. Vibók, Light-induced conical intersections: topological phase, wave packet dynamics, and molecular alignment. J. Phys. Chem. A **116**(11), 2636–2643 (2012)
30. T. Szidarovszky, G.J. Halász, A.G. Császár, L.S. Cederbaum, Á. Vibók, Direct signatures of light-induced conical intersections on the field-dressed spectrum of Na_2. J. Phys. Chem. Lett. **9**, 2739–2745 (2018)
31. T. Szidarovszky, G.J. Halász, A.G. Császár, L.S. Cederbaum, Á. Vibók, Conical intersections induced by quantum light: field-dressed spectra from the weak to the ultrastrong coupling regimes. J. Phys. Chem. Lett. **9**, 6215–6223 (2018)
32. T. Szidarovszky, A.G. Császár, G.J. Halász, Á. Vibók, Rovibronic spectra of molecules dressed by light fields. Phys. Rev. A **100** (2019)
33. S.-I. Chu, D.A. Telnov, Beyond the floquet theorem: generalized Floquet formalisms and quasienergy methods for atomic and molecular multiphoton processes in intense laser fields. Phys. Rep. **390**(1), 1–131 (2004)
34. S.-I. Chu, Recent developments in semiclassical Floquet theories for intense-field multiphoton processes, in *Advances in Atomic and Molecular Physics* (Elsevier, Amsterdam, 1985), pp. 197–253
35. S. Guérin, H.R. Jauslin, Control of quantum dynamics by laser pulses: adiabatic Floquet theory. Adv. Chem. Phys. **125**, 147–267 (2003)
36. C. Lefebvre, T.T. Nguyen-Dang, F. Dion, M.J.J. Vrakking, V.N. Serov, O. Atabek, Attosecond pump-probe transition-state spectroscopy of laser-induced molecular dissociative ionization: adiabatic versus nonadiabatic dressed-state dynamics. Phys. Rev. A **88**, 053416 (2013)
37. C. Fábri, R. Marquardt, A.G. Császár, M. Quack, Controlling tunneling in ammonia isotopomers. J. Chem. Phys. **150**, 014102 (2019)
38. A. Leclerc, D. Viennot, G. Jolicard, R. Lefebvre, O. Atabek, Controlling vibrational cooling with zero-width resonances: an adiabatic floquet approach. Phys. Rev. A **94**, 043409 (2016)
39. P.R. Bunker, P. Jensen, *Molecular Symmetry and Spectroscopy* (NRC Research Press, Ottawa, 1998)
40. S. Magnier, P. Millié, O. Dulieu, F. Masnou-Seeuws, Potential curves for the ground and excited states of the Na_2 molecule up to the (3s+5p) dissociation limit: results of two different effective potential calculations. J. Chem. Phys. **98**, 7113–7125 (1993)
41. W.T. Zemke, K.K. Verma, T. Vu, W.C. Stwalley, An investigation of radiative transition probabilities for the $A^1\sigma_u^+$-$X^1\sigma_g^+$ bands of Na_2. J. Mol. Spectrosc. **85**, 150–176 (1981)
42. T. Szidarovszky, A.G. Császár, G. Czakó, On the efficiency of treating singularities in triatomic variational vibrational computations. The vibrational states of H_3^+ up to dissociation. Phys. Chem. Chem. Phys. **12**, 8373–8386 (2010)
43. H. Xu, E. Lötstedt, A. Iwasaki, K. Yamanouchi, Sub-10-fs population inversion in N_2^+ in air lasing through multiple state coupling. Nat. Commun. **6**, 8347 (2015)
44. Y. Zhang, E. Lötstedt, K. Yamanouchi, Population inversion in a strongly driven two-level system at far-off resonance. J. Phys. B **50**, 185603 (2017)